The Mnemosyne number and the rheology of remembrance

Safa Jamali and Gareth H. McKinley

Citation: Journal of Rheology **66**, 1027 (2022); doi: 10.1122/8.0000432
View online: https://doi.org/10.1122/8.0000432
View Table of Contents: https://sor.scitation.org/toc/jor/66/5
Published by the The Society of Rheology

The Mnemosyne number and the rheology of remembrance

Safa Jamali[1,2] and Gareth H. McKinley[2,a)]

[1]*Department of Mechanical and Industrial Engineering, Northeastern University, Boston, Massachusetts 02115*
[2]*Hatsopoulos Microfluids Laboratory, Department of Mechanical Engineering, Massachusetts Institute of Technology, Cambridge, Massachusetts 02139*

(Received 30 December 2021; final revision received 8 July 2022; published 29 August 2022)

Abstract

The concept of a Deborah number is widely used in the study of viscoelastic materials to represent the ratio of a material relaxation time to the time scale of observation and to demarcate transitions between predominantly viscous or elastic material responses. However, this construct does not help quantify the importance of long transients and nonmonotonic stress jumps that are often observed in more complex time-varying systems. Many of these nonintuitive effects are lumped collectively under the term thixotropy; however, no proper nouns are associated with the key phenomena observed in such materials. Thixotropy arises from the ability of a complex structured fluid to remember its prior deformation history, so it is natural to name the dimensionless group representing such behavior with respect to the ability to remember. In Greek mythology, Mnemosyne was the mother of the nine Muses and the goddess of memory. We, thus, propose the definition of a Mnemosyne number as the dimensionless product of the thixotropic time scale and the imposed rate of deformation. The Mnemosyne number is, thus, a measure of the flow strength compared to the thixotropic time scale. Since long transient responses are endemic to thixotropic materials, one also needs to consider the duration of flow. The relevant dimensionless measure of this duration can be represented in terms of a mutation number, which compares the time scale of experiment/observation to the thixotropic time scale. Collating the mutation number and the Mnemosyne number, we can construct a general two-dimensional map that helps understand thixotropic behavior. We quantify these ideas using several of the simplest canonical thixotropic models available in the literature. https://doi.org/10.1122/8.0000432

I. INTRODUCTION

In 1964, Marcus Reiner [1] during an after-dinner talk at the 4th International Congress on Rheology introduced the core rheological concept of the Deborah number (*De*) as a ratio of time scales; specifically the relaxation time of the material of interest as compared to the time scale of observation. The concept became central to the rheology community very quickly, and decades later, we commonly compare and contrast different time scales associated with rheological features of different linear viscoelastic material systems through this ratio, as well as other dimensionless groupings that quantify the additional (nonlinear) responses of more complex materials. For instance, in polymeric systems and processing flows, the Weissenberg number (*Wi*) provides an indication of how important nonlinear rheological effects such as normal stress differences are in the material response of a complex fluid [2,3], while the Reynolds number (*Re*), familiar to many from fluid mechanics, provides a relative measure of fluid inertia to viscous stresses. Both of these latter parameters depend on the imposed flow strength; however, their ratio *Wi/Re* (commonly referred to as the elasticity number, *El*) is independent of the flow rate and provides a measure of the relative importance of viscoelastic stress relaxation to the viscous diffusion time [4]. Such designations help in probing the role of flow without changing the material properties. For instance, one can change the Reynolds number and independently discuss the elastic effects. When considering suspensions under flow, one can compactly represent the rheological behavior with respect to the ratio between the rates of advection to the rate of diffusion, resulting in the Péclet number (*Pe*) [5]. One could argue that *Wi* and *Pe* both represent the ratio of the strength of the flow compared to the natural time scale for evolution of the material's [micro]structure, whether driven by viscoelastic relaxation or Brownian diffusion. In more complex attractive particulate systems, the Mason number (*Mn*) formed from the ratio of viscous shearing forces to attractive interparticle forces again provides an effective dimensionless group to represent the quasisteady state rheology of colloidal gels. Once again, the ratio of these two parameters, commonly denoted $\lambda = Pe/Mn$, is dimensionless and independent of flow strength and provides a relative measure of how strong interparticle attractions are compared to the randomizing forces of Brownian motion. It is interesting to note that in both of these examples no proper names are associated with the (dimensionless) ratios of two (eponymous) dimensionless product groups.

While these dimensionless groups have been extremely useful and important in categorizing the different regimes of material response observed in complex fluids and in confronting rheometric data with the predictions of appropriate constitutive models, they cannot help us in quantifying or describing the long transients and nonmonotonic stress

a)Author to whom correspondence should be addressed; electronic mail: gareth@mit.edu

jumps observed in other more-complex time-varying systems. Many of these confusing and nonintuitive effects are lumped collectively under the term *Thixotropy* and its antonym *Rheopexy* (*or anti-thixotropy*). This vast field has been reviewed extensively and authoritatively (see, for example, [6–13]); however, no proper nouns are commonly associated with key phenomena or underlying physical processes observed in such materials. This is perhaps due to conflation with a plethora of other rheological phenomena, such as dilatancy, shear-thinning, and viscoelasticity with thixotropy, which muddied the development of the field [14].

The term thixotropy was originally coined in 1927 by Peterfi [15], combining the Greek words *thixis* (stirring or shaking) and *trepo* (turning or changing), to describe the ability of living cells to regain their original solidlike state during a period of rest, after first being driven into a liquidlike state by agitation (a process we would now more appropriately refer to as *rheological aging*; see, for example, the clear discussion in [10], and a historical perspective in [16,17]). Virtually all other early accounts of thixotropic behavior have to do with the sol-gel transition, and the ability of particulate gels to resolidify (due to interparticle interactions) after becoming completely liquefied under flow [18–20]. As described in [16], some of these thixotropic effects can be discussed in the context of "aging" and "rejuvenation" of structured fluids. Nonetheless, aging commonly refers to restructuration of a fluid under quiescent conditions. Thixotropy, however, emerges under nonzero imposed deformation rates, and as such it is important to discuss thixotropic effects under flowing conditions.

In Larson's review [9] of thixotropic constitutive models, a clear definition and a distinction are presented for thixotropy vs nonlinear viscoelasticity: "*a time-dependent viscous response to the history of the strain rate, with fading memory of that history*." The concept of "*fading memory*" was first introduced in the context of viscoelasticity by Coleman and Noll [21]. Note that although Coleman and Noll described fading memory with respect to viscoelastic constitutive models, the very same concept can be associated with thixotropic memory; indeed, when viewed from a continuum mechanics perspective there is no distinction. However, when discussing the memory effects, distinctions can be drawn from a microstructural perspective (albeit not necessarily appearing in the constitutive description of the system), by distinguishing formation and fading of the memory caused by convective processes and the imposed flow, referred to as the "*kinematic memory*," versus the viscoelastic memory of a polymer chain or other deformed macromolecular structure as a tendency to relax (or recoil) toward a maximum entropy configuration. In a sequel review [10], Larson clearly notes that few, if any, fluids may exhibit purely thixotropic behavior and that thixotropy commonly co-exists with viscoelasticity, and it can be difficult to clearly separate the two effects. Nonetheless, here we also adopt a similar definition as Larson for ideal thixotropy, as a reversible, inelastic, time-dependence of the viscosity (and/or a shear yield stress) during and after flow. From a thermodynamic perspective, descent toward an energy minimizing state can be driven by enthalpic and/or entropic effects. One could argue that in primarily viscoelastic fluids, e.g., polymer solutions, it is maximization of a polymer chain's entropy that drives the microstructural dynamics and, thus, the viscoelastic stress relaxation of the fluid in general. In contrast, for essentially thixotropic fluids, e.g., attractive colloidal gels, finding local/global energy minima is controlled by directly reducing the potential energy of the colloidal assembly through particle-particle interactions. This provides a contrast between the underpinnings of viscoelasticity and thixotropy: viscoelastic effects emerge from microscopic (single particle/chain level) configurations and are, hence, commonly associated with shorter time scales, while thixotropic effects originate from mesoscopic (cluster/multiparticle level) rearrangements of the structure that naturally evolve over longer time scales.

A common rheological probe of thixotropy is often taken to be the appearance of hysteresis in an up/down stress (or rate) sweep, the so-called *Thixotropic Loop* (see, for example, [14] or [22]) However, such hysteresis loops can result from a number of different physical origins. In groundbreaking early work, Bird and Marsh [23] showed that a variety of distinct hysteresis loops can be generated using slowly varying shear flow protocols with the nonlinear viscoelastic models available at the time. Even earlier, Fredrickson [24] (Chapter 6, Viscoelastic Substances) demonstrated that hysteresis signals can even be generated using an up/down ramp of the linear Maxwell model if unsteady inertial effects and the propagation of shear waves across the rheometer gap are considered. It is worth noting that although the effects of viscoelasticity can manifest in qualitatively similar hysteretic signatures as thixotropy, the two behaviors can often be distinguished pragmatically by differences in magnitudes and time scales. That is, the inherent separation in microstructural length scales described above often translates into viscoelastic (entropic) memory effects being demonstrated over a few strain units, and thixotropic (kinematic) memory effects occurring over tens or hundreds of strain units. Although in most real-world industrial complex fluids (e.g., formulated paints and inks containing polymers, surfactants, and colloidal pigments), a wide spectrum of length and time scales may be important, as Larson states in [10], "*it is a matter of pragmatic judgment whether a real material's behavior is close enough to the ideal to warrant a particular terminology*."

Through the careful design of a suitable rheometric protocol (which we discuss at more length later), Divoux and co-workers [25] showed that the fading response of a fluid to the history of deformation can, in fact, be characterized by a thixotropic time scale (which they identify as θ but henceforth we shall denote τ_{thix} to be more consistent with SOR nomenclature), on which the material shows the most pronounced sensitivity to the history of the deformation rate. Just as real viscoelastic fluids typically exhibit a spectrum of relaxation times, a typical thixotropic material may also show a range of thixotropic time scales [26]; however here, for simplicity, we assume that (just as in modeling of polydisperse viscoelastic responses) this distribution can be adequately and compactly represented by an appropriate moment or average of the underlying thixotropic time-scale spectrum.

There has been a re-awakening and growth of interest in thixotropy over the past few years, most probably because of its ubiquity in many real commercial systems. A concise but comprehensive summary of recent developments in the constitutive modeling of such systems has been given recently by Varchanis *et al*. [27]. Ewoldt and McKinley [28] have also discussed three-dimensional phase map representations for thixotropic elasto-visco-elastic (TEVP) materials, in which plastic and viscoelastic behavior can be simultaneously observed with thixotropy; however, the lack of a clear and definitive nomenclature for the dimensionless groups to be used for parameterizing the magnitude of each effect results in ungainly terms such as the *thixoviscous (TV) number* and *thixoplastic (TP) number*. The goal of this article is to propose suitable names for these dimensionless groups that can then be used by the rheology community to conceptually represent and discuss different aspects of thixotropic behavior in a clear and unambiguous manner. As such, recognizing that thixotropy and viscoelasticity have similarities in their rheological signatures, we intend to propose a series of dimensionless groups, as well as flow protocols, that target thixotropic effects specifically.

II. MNEMOSYNE: THE GODDESS OF MEMORY

Astutely, when proposing the concept of the Deborah number to quantify phenomena being observed and reported in a dynamically evolving field, Reiner avoided association with living rheologists, and we take the same approach here. We recognize that every thixotropic (or antithixotropic) effect observed in a complex fluid is owed to its ability to remember the history of its previous deformation. Hence, it is natural to name the dimensionless group representing such behavior with respect to the ability to remember. In Greek mythology, *Mnemosyne* was one of the *Titans*, and the goddess of memory and remembrance. She presided over a river (or a spring) that flowed in parallel to the river of *Lethe*, the embodiment of forgetfulness. The dead, before reincarnation, drank water from the river Lethe to forget their past, in contrast to the idea of drinking from the Mnemosyne for novices in the Orphico-Pythagorean brotherhood [29]. In contemporary language, we use the term *mnemonic* to refer to an artifact or device to help us remember a key concept or result. We, thus, propose to define the *Mnemosyne number* as the dimensionless product of the appropriately defined thixotropic time scale of a material and the imposed rate of deformation: $My = \tau_{thix}\dot{\gamma}$. We propose the abbreviation *My* to avoid any confusion with the Mason number (*Mn*) that is already used in studies of colloidal gels. In any given kinematic situation, a high value of *My* indicates the potential for pronounced thixotropic memory of previous flow conditions and, thus, we expect the Mnemosyne number to capture (at least in part) a suitable measure of the extent of thixotropy in a system.

The value of the Mnemosyne number allows us to clearly distinguish thixotropic phenomena from other rheological responses; and any rheometric test or processing flow of interest may correspond to vanishingly small values of *Re*, *De*, and/or *Wi*, but a finite (and perhaps large) value of *My*. For instance, in shearing of carbon black or clay suspensions, nonlinear viscoelastic effects (such as normal stress differences) are typically much smaller in magnitude and less important than thixotropic transient responses in the shear stress, so $Wi \ll My$. The ratio $Wi/My = \tau_{el}/\tau_{thix}$ has been previously referred to as a *thixoelastic parameter* by Ewoldt and McKinley [28] and helps distinguish whether nonlinear elastic effects are more important ($Wi/My \gg 1$) or thixotropic/aging effects dominate ($Wi/My \ll 1$). Experimental protocols for distinguishing such effects have recently been considered by Agarwal *et al*. [13]. We do not seek to rename this quotient because, like the quantities *Wi/Re* and *Pe/Mn* discussed above, it is a deformation-rate-independent quantity formed from the ratio of two extant, and already named, dimensionless parameters.

The Mnemosyne number, as defined here, is a measure of flow *strength* compared to the thixotropic time scale. However, because of the long transient responses endemic to thixotropic materials, one also needs to consider the *duration* of any flow protocol in order to determine how large the magnitude of the actual thixotropic rheological response is. In dealing with many thixotropic materials, the experimental protocol commonly involves a preshearing state at large deformation rates for a carefully prescribed period of time in order to erase the material's memory of its previous flow history (e.g., the initial trauma of loading it into a rheometer). It is appropriate, thus, to refer to this preshearing process as "*letherizing*" the material sample, as the memory of its previous life(s) is forgotten. For instance, in order to fully letherize a thixotropic sample, *strong flows of long duration* are required. Note that as opposed to a kinematic definition of a strong vs weak flow (in terms of a positive Lyapunov exponent and the exponential stretching of material elements), within the context of thixotropy the term "strong flow" corresponds to ones for which $My \gg 1$. The relevant duration of a flow or rheometric test protocol (which we denote for clarity as t_{exp}) for a time-evolving material has been considered quite generally by Mours and Winter [30], and they argue that this can be represented in terms of a *mutation number*: $Mu = t_{exp}/\tau_{thix}$, which compares the duration of the experiment/observation to the time scale characterizing the rate of change of the material (here the thixotropic time scale τ_{thix}). For example, in order to ensure that a viscoelastic fluid does not change its properties significantly or evolve during a typically oscillatory test (for which the duration is $t_{exp} \approx 2\pi/\omega$) we require $Mu \ll 1$. This constraint has prompted the development of new fast oscillatory shear test protocols such as the Optimized Windowed Chirp [31].

III. MUTATION-MEMORY MAPS

Combining these considerations regarding both the strength and the length of a specific shearing protocol, it becomes clear that the Mnemosyne number and the mutation number can be used to construct a general two-dimensional map of thixotropic behavior as shown schematically in Fig. 1. First, we note that during a specific time-dependent flow protocol (e.g., start-up of steady shear flow), the product of these two dimensionless groups gives a measure of the

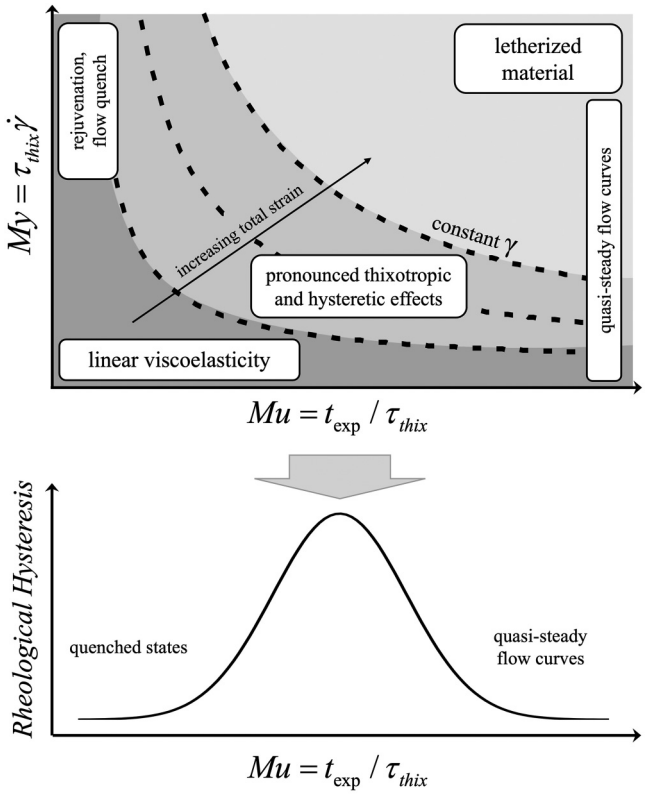

FIG. 1. A proposed phase map for representing, locating, and understanding common rheological phenomena associated with rheological characterization of thixotropic materials in terms of the Mnemosyne number, *My* and the mutation number, *Mu*. The lower figure shows a generic measure of the nonmonotonic evolution rheological hysteresis (see the text for suggested definition) as a function of the experimental duration (or mutation number) of the experiment.

total accumulated strain: $My.Mu = (\tau_{\text{thix}} \cdot \dot{\gamma})(t_{\text{exp}}/\tau_{\text{thix}}) = \gamma$, as indicated by the broken hyperbolic lines. Low strains correspond to the lower left and large strains to the upper right of this operating space. We now consider the physics captured in different quadrants of this thixotropy map. The viscoelastic response of a TEVP material can be reliably measured using weak flows of (relatively) short duration located in the lower left of the map ($Mu \ll 1$, $My \ll 1$). Here, thixotropic changes to the material as well as the total shearing deformation imposed are rather small and the sample does not mutate during the experimental test. In contrast, very strong and long flows in the upper right ($Mu \gg 1$, $My \gg 1$) are used to letherize the material into a fluid-like behavior and eradicate all memory of the previous states of the material.

At the heart of this map at intermediate total strains lie regions with pronounced thixotropic and hysteretic effects. This is the region where long-duration—and frequently confounding—transient dynamical responses such as nonmonotonic stress evolution and/or transient shear banding are observed. We explore this regime in greater detail below. To the far right of this figure at small *My*, and large *Mu*, (corresponding to weak thixotropic effects and longer observation times), one can recover the quasi-steady flow curve of a material, provided the accumulated strain is also large enough that the system evolves (or mutates) toward its steady flowing state. Conversely, very large values of *My* and very small *Mu* (corresponding to the upper left of Fig. 1) correspond to the process of quenching a time-dependent thixotropic material into a nonequilibrium (often glassy or nonequilibrium gel) microstructure.

Finally, for completeness, we note that other time-dependent effects such as "rheological aging" of glassy materials are possible even under rest (no imposed flow) conditions. These effects are clearly distinguished from thixotropy by Wei and Larson (see Sec. II B of [10]). Such phenomena (corresponding to $\dot{\gamma} = 0$) evidently cannot be uniquely represented as coordinate points on a two-dimensional map of the form of Fig. 1 and would necessitate a more complex (but straightforward) three-dimensional representation, which we do not pursue further here. The dynamic rheological process commonly known as "rejuvenation" would correspond to projection of a material's coordinates from high (i.e., "old") values of this third (as yet unnamed) material age axis back to low values characteristic of a rheologically young material.

As we have depicted schematically in the lower part of Fig. 1, quantitative measures of the *rheological hysteresis* that arises during shearing of a thixotropic material are expected to be a function of the time scale of the experimental test protocol (or, equivalently, the mutation number *Mu*) and will be most pronounced in intermediate strain/time regimes. To generate quantitative and reproducible thixotropic data to map out this nonmonotonic hysteresis curve, it is essential to first develop a robust rheometric test protocol. Early experimental iterations of specialized instruments such as the *Thixotrometer* of Pryce-Jones [32] often used "thixotropic loops" starting from rest conditions and first increasing (and then decreasing) the imposed shear rate (or shear stress) and are reviewed in detail by Bauer and Collins [14]. However, for many structurally sensitive commercial systems, as well as model colloidal "soft glassy" materials, the initial state of the sample is a strong function of the loading/preparation history, as well as the waiting time t_w before the experiment is performed. This can make it hard to achieve repeatable and device-independent data. Mewis [7] has argued convincingly for the adoption of "step rate" tests (in which the shear rate on the material is jumped rapidly from a low value to high value or vice versa). Performing a series of such step-rate tests provides a rich dataset that indeed maps out the functional describing the entire thixotropic material response envelope but can be extremely time-consuming to generate and analyze. In a very recent paper, Choi *et al.* [33] used a series of stress jump experiments and mapped thixotropic behavior to distinguish between elastic and viscous contributions to the total fluid stress.

Recently, Divoux and co-workers [25,34] have described a somewhat simpler but robust ramp-down/ramp-up flow protocol that provides the data density required to probe the spectrum of thixotropic responses in a material in a more efficacious way. One begins in the upper right of Fig. 1 at an initially large shear rate, $\dot{\gamma}_i$, corresponding to a *fully letherized* material (thus generating a repeatable and history-independent initial configuration) and then imposes a series of different shear rates down to a final minimum shear rate, $\dot{\gamma}_f$ before

reversing the process and returning back to the initial (large) shear rate. These down/up ramps may consist of a series of n discrete steps, each of length Δt (as utilized in [25] so that the total elapsed time is $t_{\text{exp}} = n\Delta t$) or, perhaps more conveniently, a single continuously varying ramp down at a specified rate, r. This continuous ramp could also be chosen to be linear, or a power-law or exponential in character. In recent dissipative particle dynamics (DPD) computations with an attractive colloidal system [35,36], we have shown that although the precise numerical values of the computed hysteresis measure will change for each ramp protocol, the qualitative features of this protocol are very robust and quite generally of the nonmonotonic form sketched in Fig. 1.

In Fig. 2, we illustrate a number of different possible protocols, namely, a step-wise (blue solid line) and a continuous ramp down/up (red broken line), a single step jump or "quench" protocol to a low final shear rate (orange dashed curve) and finally a simple start-up of steady shear flow protocol (as shown by the green dotted step function) at an arbitrary deformation rate. The top figure depicts the temporal variation in the applied deformation rate of these different protocols for a given (constant) experimental duration Δt_{exp}, while the bottom figure shows the corresponding graph mapped onto the *Mu–My* diagram with direction indicated by an arrow. Different levels of shading/transparency increments show different (increasing) values of Δt_{exp}. Note that the initial departure point on the *Mu–My* diagram for each of these protocols is selected to always lie within the fully letherized state (so that all previous

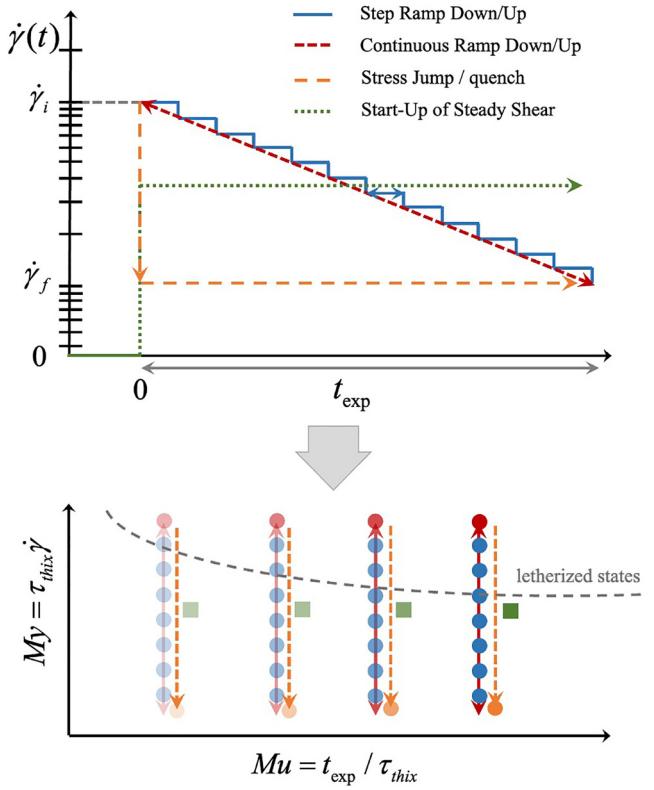

FIG. 2. The time-varying shear rate as a function of time for a given Δt_{exp} for different flow protocols (top), and the corresponding values mapped onto the proposed *Mu–My* diagram. Different color transparencies indicate different values of Δt_{exp}.

deformations have been forgotten). The stress jump and quench, step-wise, and continuous ramp protocols for a given Δt_{exp} are indistinguishable on this diagram. Thus, for illustration purposes, different circular points indicating different values of the prescribed shear rate steps are shown on top of the continuous line for ramp down/up protocols, and a dashed line (with no intermediate points and just a final state at $\dot{\gamma}_{\text{min}}$) is presented for the stress jump/quench protocol. In contrast, the start-up of steady shear experiments (shown by green squares) is represented by a series of horizontal points on the *Mu–My* diagram, as the applied shear rate (and, thus, the Mnemosyne number) is constant throughout, and the experimental time that enters the numerator of the mutation number increases monotonically with the time of shearing. It is important to note that the entire *Mu–My* space can still be explored using this protocol by performing a series of start-up experiments at different values of the imposed shear rate—corresponding to a series of horizontal sweeps through this *Mu–My* parameter space.

For didactic simplicity, we only consider in detail here a linearly varying shear rate $\dot{\gamma}(t) = \dot{\gamma}_i - rt$ performed at a (user-selectable) rate r. The total time of the down-ramp experiment is then $t_{\text{exp}} = (\dot{\gamma}_i - \dot{\gamma}_f)/r$ and consequently the kinematic history of the down-ramp test can also be written as $\dot{\gamma}(t) = \dot{\gamma}_i - (\dot{\gamma}_i - \dot{\gamma}_f)(t/t_{\text{exp}})$. A typical protocol may select $\dot{\gamma}_i = 100\,\text{s}^{-1}$ and $\dot{\gamma}_f = 1\,\text{s}^{-1}$, followed by an up-ramp with the initial and final shear rate values interchanged. As proposed by Divoux *et al.* [25] and adapted by [34–36], an appropriate measure of the rheological hysteresis arising from thixotropy is then the difference in areas under the apparent (nonequilibrium) flow curve of $\sigma(\dot{\gamma})$ measured on the up/down trajectories,

$$A_{\Delta\sigma} = -\int_{\dot{\gamma}_f}^{\dot{\gamma}_i} \sigma^{(\text{down})}\, d\,\log\,\dot{\gamma} + \int_{\dot{\gamma}_f}^{\dot{\gamma}_i} \sigma^{(\text{up})}\, d\,\log\,\dot{\gamma}$$
$$\equiv \int_{\dot{\gamma}_f}^{\dot{\gamma}_i} \Delta\sigma(\dot{\gamma}) d\,\log\,\dot{\gamma}, \tag{1}$$

where $\Delta\sigma(\dot{\gamma}) = \sigma^{(\text{up})} - \sigma^{(\text{down})}$ and can, in principle, be positive or negative (for an antithixotropic material). To avoid ambiguity and focus on the magnitude of the hysteretic effects, we follow [25] and use the absolute magnitude of the stress difference, $|\Delta\sigma(\dot{\gamma})|$, in up/down ramps. In this formalism, the shear rate is logarithmically spaced so that an equal weight is given to low and high shear rates [25]. Nonetheless, the hysteresis area as defined in Eq. (1) is not dimensionless and we, therefore, normalize the hysteresis area by the area under the ramp-down flow curve (also schematically shown in the bottom right sketch of Fig. 3), resulting in the following definition of a *dimensionless* hysteresis measure that captures the extent of thixotropy in a material,

$$\tilde{A}_\sigma = \frac{\int_{\dot{\gamma}_f}^{\dot{\gamma}_i} |\Delta\sigma(\dot{\gamma})| d\,\log\,\dot{\gamma}}{\left|\int_{\dot{\gamma}_f}^{\dot{\gamma}_i} \sigma^{(\text{down})}\, d\,\log\,\dot{\gamma}\right|}. \tag{2}$$

One could alternatively nondimensionalize the hysteresis area defined in Eq. (1) by scaling the shear stress values by a

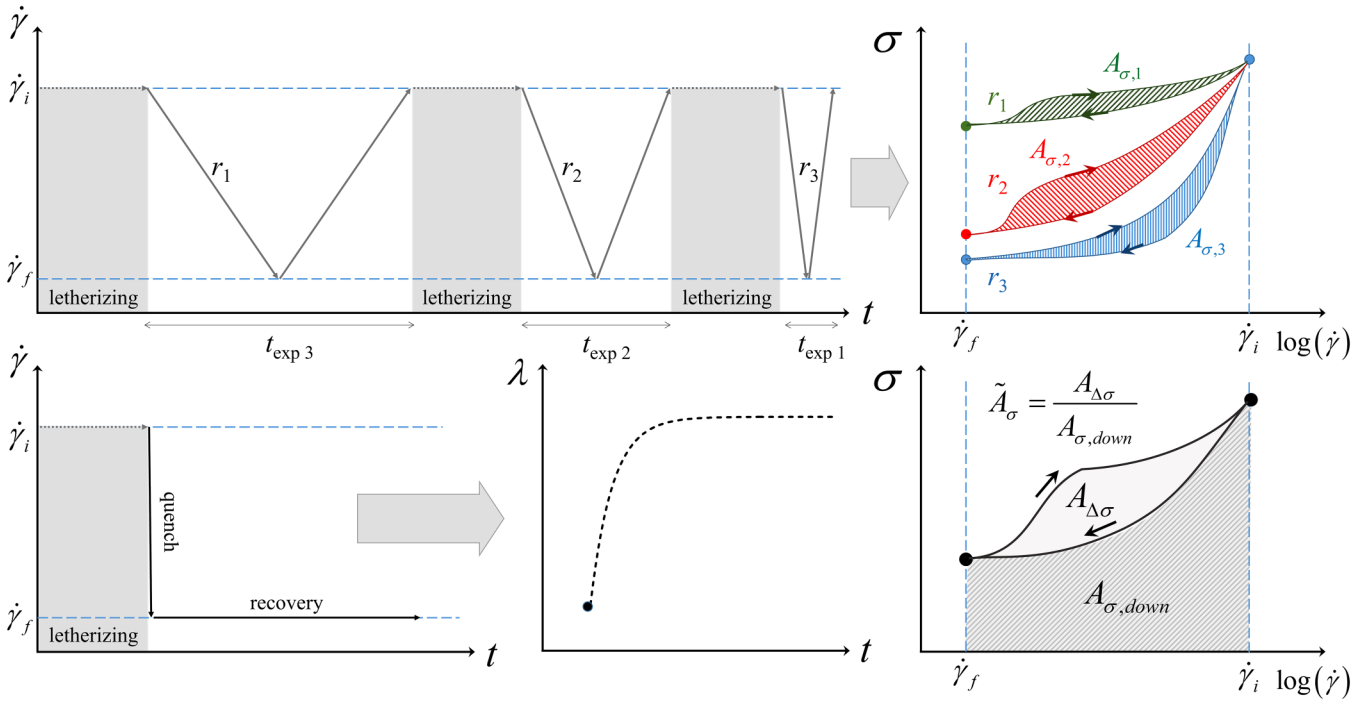

FIG. 3. An example of: (top) a repeated up/down ramp protocol, and (bottom) a shear rate (or shear stress) jump experiment, for probing rheological hysteresis and identifying the thixotropic time scale of a material. The quench experiment provides a convenient protocol for monitoring the recovery of the material [as represented here schematically by the evolution in a scalar structural parameter $\lambda(\dot{\gamma}, t)$]. Between each ramp r_k ($k = 1, 2, 3,\ldots$), a letherizing period at high shear rate ($\dot{\gamma}_i$) rejuvenates the material. The high value of the initial Mnemosyne number My_i ensures elimination of any shear-induced structure (SIS) formation, and monitoring the time-invariance of $\sigma(\dot{\gamma}_i)$ also allows us to check that no long-term irreversible effects such as sample drying or progressive shear-induced sample degradation are in play. On the right we have sketched the corresponding apparent flow curves $\sigma(\dot{\gamma}; r)$ that might be expected for a thixotropic material with a yield stress (for a recent example, see [37]), but the existence of a yield stress in the thixotropic material is not essential.

yield stress σ_y and normalizing the shear rate values by $\dot{\gamma}_f$; however, not all thixotropic fluids exhibit a yield stress, and even for the ones that do, from an experimental point of view the precise value of the yield stress is not necessarily always clear (and may vary with the protocol used to measure it). By imposing a series of different up/down ramp rates r_k (for $k = 1, 2, \ldots, N$) as shown schematically in Fig. 3, we can then systematically map out the (typically) nonmonotonic evolution of the hysteresis area in the apparent flow curve $\sigma(\dot{\gamma}(t; r))$ and identify the characteristic thixotropic time scale τ_{thix} of the test material. One can define the thixotropic time scale τ_{thix} as the peak of the hysteresis area when plotted against the time interval of the experiment as suggested by Divoux *et al.* [25]. Nonetheless, to avoid unambiguity, and for consistency, we define the thixotropic time scale τ_{thix} to be the time scale required for a full recovery of shear stress (and hence microstructure) upon a stress jump experiment from an initially large deformation rate, $\dot{\gamma}_i$, to a nonzero small rate of $\dot{\gamma}_f$. For very long duration experiments (with large values of t_{exp}), the quasistatic nature of the experiment means that the equilibrium flow curve is obtained with little/no hysteresis. However, as the ramp rate down/up is increased, the experimental duration becomes progressively shorter, and rheological hysteresis becomes significant, if the sample is thixotropic. Additionally, one should note that for controlled stress experiments similar descriptions as in Eqs. (1) and (2) can be written based on the overall (measured) values of the deformation rates at the beginning and end of the ramp. However, in the case of yield stress fluids, sweeping stresses down (below a dynamic yield stress) and subsequently up (above a static yield stress) can result in even more complex hysteretic loops and, thus, distorted measurement of a thixotropic time scale. Thus, here we will focus on controlled rate experiments, which result in well-defined closed-loop hysteresis curves.

This time-varying deformation protocol is, thus, another example of *mechanical spectroscopy*, in the same way that (for a nonmutating, viscoelastic material) imposing a sequence of different oscillatory deformation frequencies (either as a set of discrete frequencies with $\tau_{\text{exp}} \approx 2\pi/\omega$ or in a single, time-varying "chirp" waveform) probes different well-defined states—such as the terminal regime (at low frequencies) and the rubbery plateau (at high frequencies)—as well as enabling determination of the full relaxation spectrum of the material. Similarly, orthogonally superposed chirp waveforms can be devised as a fast probe of the rheological response in rapidly mutating complex fluids [38].

Very rapid ramp rates down from $\dot{\gamma}_i$ are akin to mechanically "quenching" the microstructure of the material in its fully letherized (shear-rejuvenated) state. A useful analogy here is the rapid thermal quenching of molten metals in order to form metallic glass states with markedly different mechanical properties, as compared to slowly cooled "equilibrium" microstructures that commonly feature polycrystalline domains. Recent simultaneous measurements of microstructure or conductivity and dynamic modulus in carbon black pastes being developed for battery slurries have also illustrated the variety of nonequilibrium states that can be

developed in thixotropic microstructured materials [39]. Our previous simulations of attractive colloidal gels also show clearly that the microstructure and moduli of a quenched gel can be quite different from slowly gelled samples [35]. As such, the linear viscoelastic regimes that also cover the quenched samples may or may not represent an equilibrium state for the microstructure. However, letherized states in the *Mu–My* map of Fig. 1 will always correspond to equilibrium states of the microstructure. Of course, we must bear in mind that some complex fluids may have such short thixotropic time scales that it is not possible (within the limitations of current rheometers) to quench the structure fast enough to explore the full nonmonotonic curve of $A_\sigma(r)$. This seems to be the case for carefully prepared Carbopol samples which have a thixotropic time scale of less than one second [25] and, thus, always reside toward the far right of Fig. 1. Similarly, we may never be able to shear a material strongly enough to fully letherize it and completely eliminate memory of its previous lives (see the discussion in Sec. II D of [10]). Regardless of the choice of flow protocol adopted for quantitative measurement of thixotropic time scale, one would argue that once this time scale is measured, *Mu–My* diagrams such as the one sketched in Fig. 1 can be used to describe different flow regimes, as one axis describes the strength of flow and the other one the time of observation. Pipkin diagrams are based on similar principles and have been used consistently for understanding nonlinear viscoelastic material responses.

IV. RHEOLOGICAL HYSTERESIS IN COMMON MODELS FOR THIXOTROPY

Finally, we note that this framework is also of use in understanding the response of constitutive equations written for thixotropic materials. Virtually all inelastic constitutive equations, beginning with the expression proposed by Goodeve [40] to enhanced variants such as those discussed by Coussot *et al.* [41], to other variations of elastoplastic constitutive models such as Acierno's model [42], and detailed phenomenological elastoviscoplastic models such as the Isotropic-Kinematic Hardening (IKH) model [43–46], resort to a description of the evolution in one (or more) scalar thixotropy parameter(s), $\lambda(t; \dot{\gamma}(t'))$, which capture some appropriately weighted and normalized measure of the evolving distribution in the microstructural states within the material. Some recent efforts have shown that viscoelastic models can also be used to augment the range of thixotropic effects described [33,47]. The evolution in this thixotropy parameter then controls the bulk rheological response of the material. Early computational explorations of this form (including up/down hysteresis loops) can be found in the pioneering work of Frederickson [48].

A detailed review of different constitutive models for thixotropic fluids is provided in [9]. In the simplest generic form, one can construct a time-evolving functional for this structural parameter that might be written generically as

$$\frac{d\lambda}{dt} = \frac{1}{\tau_{\text{thix}}}(1-\lambda) - \beta\lambda\dot{\gamma}. \tag{3}$$

The first term on the right describes "creation" or rebuilding of microstructure, while the second is a shear-rate-dependent destruction term. The buildup rate is determined by the characteristic thixotropic time of the material, and β is a (material-dependent) dimensionless parameter describing how effectively the microstructure is broken down under shear. A simple steady-state solution of such an equation (at a given deformation rate) yields $\lambda = 1/(1+\beta\, My)$, clearly illustrating the role of the Mnemosyne number in quantifying changes in the microstructural state and (ultimately) the bulk rheology of a thixotropic material under shear. A full time-dependent solution of Eq. (3) for a time-varying up-down ramp $\dot{\gamma}(t; r)$ corresponds to a vertical trajectory through the state map in Fig. 1; starting at the top (i.e., at a high initial shear rate with $My_i \gg 1$) and moving first down (i.e., a ramp down in shear rate to a final value $\dot{\gamma}_f$ with $My_f \ll 1$) and then back up (i.e., a ramp up in shear rate). The specific value of *Mu* for this test is set by the specified ramp rate *r*. The degree of hysteresis measured (or computed) during this down/up ramp will of course depend on the ramp rate *r* and the specific form of the thixotropic constitutive model under consideration (of which there are myriad; see, for example, the discussion/review of Varchanis *et al.* [27] or [47]).

Here, for illustrative purposes, we have performed a simple numerical investigation of the flow protocol mentioned above, $\dot{\gamma}(t) = \dot{\gamma}_i - (\dot{\gamma}_i - \dot{\gamma}_f)(t/t_{\text{exp}})$, with Eq. (3) governing the time evolution of the thixotropy parameter, $\lambda(t; \dot{\gamma}(t))$. One then can select or construct different constitutive equations for the stress response of the fluid under such flow protocols. We present three simple limiting cases of some canonical thixotropic constitutive equations:

(i) An inelastic *thixoviscous (TV) fluid* in which the shear stress response to an applied deformation rate is given by $\sigma(t) = [\eta_s + \eta_p\lambda(t; \dot{\gamma}(t))]\dot{\gamma}(t)$. Here, the total viscosity of the thixotropic material is written as a sum of contributions from an invariant background Newtonian solvent viscosity, η_s, and from the evolving structural viscosity, $\eta_p\lambda(t)$.

(ii) A *thixoplastic (TP) fluid* with the constitutive equation is given as $\sigma(t) = \sigma_y\lambda(t; \dot{\gamma}(t)) + \eta_s\dot{\gamma}(t)$, for which the value of the yield stress, σ_y, depends on the level of structure in the material but the plastic shearing viscosity remains constant.

(iii) A *thixo-visco-plastic* (TVP) *fluid* (which might also be referred to as a thixotropic yield stress fluid or TYSF [29]) that takes a constitutive form combined from (i) and (ii) as $\sigma(t) = \sigma_y\lambda(t; \dot{\gamma}(t)) + [\eta_s + \eta_p\lambda(t; \dot{\gamma}(t))]\dot{\gamma}(t)$. For a TVP fluid, the evolution of the microstructure characterizing the material directly changes the yield stress as well as the plastic viscosity of the fluid.

Of course, there are a myriad of other functional forms, some of which have been developed to include the role of elasticity as well [43,46,49]; however, here, we focus on a simple class of inelastic models with no elastic response. Note that for all three formulations examined here, a material with no microstructure, $\lambda = 0$, corresponds to a simple Newtonian rheology. In the numerical calculations described below, we fix the value of the yield stress at $\sigma_y = 20\,\text{Pa}$, the

Newtonian viscosity at $\eta_s = 1\,\mathrm{Pa\,s}$ and the structural viscosity at $\eta_p = 4\,\mathrm{Pa\,s}$ to be broadly consistent with the carbon black gels considered by Helal *et al.* [39]. Finally, for illustrative purposes, we set $\tau_{\mathrm{thix}} = 10\,\mathrm{s}$ consistent with the results of Divoux *et al.* [25]. The transient solution for the evolution in the thixotropy parameter [Eq. (3)] is independent of the choice of stress constitutive equation and is presented in Fig. 4 for a prototypical choice of $\beta = 0.1$ and a very wide range of experimental durations varying from 10^{-2} to $10^{6}\,\mathrm{s}$. The solid lines represent the ramp-down flow from the initial shear rate of $\dot{\gamma}_i = 100\,\mathrm{s}^{-1}$ to the final shear rate of $\dot{\gamma}_f = 0.1\,\mathrm{s}^{-1}$ and the dashed lines represent the ramp-up protocol back to the fully letherized or destructured state (often also referred to as "shear melting"). There are many features that are clearly evident in the thixotropic structural evolution curves shown in Fig. 4. First, one can immediately identify hysteresis loops as the ramp up/down curves do not collapse onto each other for intermediate experimental durations. For very short flow durations, $Mu \approx 0$, the material does not have sufficient time to build up structure and, thus, λ remains virtually null for the duration of the experiment, resulting in a negligible hysteresis area. On the other hand, for very long experimental durations, $Mu \gg 1$ and for each instantaneous shear rate, the thixotropy parameter evolves to its quasisteady state value. Thus, the hysteresis area is minimal or nonexistent for this regime as well. The parameter β directly controls the effectiveness of shear flow in breaking up the structure and, thus, controls the quasisteady state value of λ to be $\lambda(t) \approx 1/(1 + \beta\tau_{\mathrm{thix}}\dot{\gamma}(t)) = 1/(1 + \beta My(t))$. For our choice of parameters, this yields $\lambda_f \approx 0.9$ at the end of the ramp down phase [when $\beta My(t_f) = \beta\tau_{\mathrm{thix}}\dot{\gamma}_f = 0.1$], consistent with the results shown in Fig. 3.

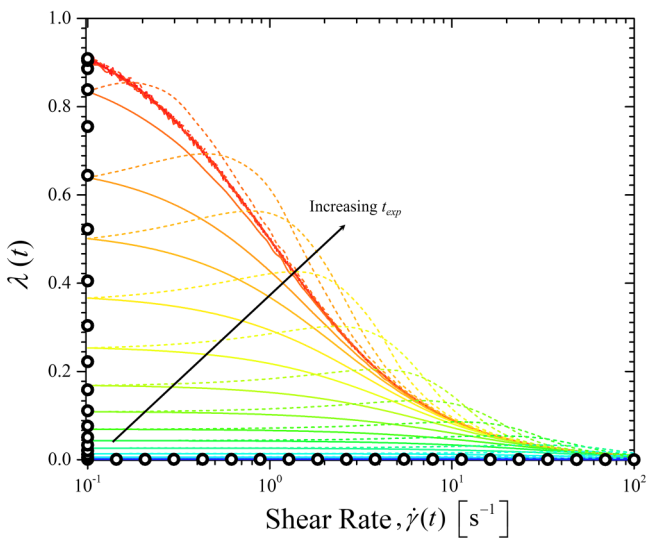

FIG. 4. Numerical solution of Eq. (3) for time evolution of the thixotropy parameter, $\lambda(t, \dot{\gamma})$, under a linear ramp down/up flow protocol as shown schematically in Fig. 3. The color increments from blue to red represent (see color version online, and indicated in print by the direction of the arrow) represent progressively longer total times of experiments, t_{exp}, corresponding to different mutation numbers ranging from $Mu = 10^{-3} - 10^{5}$. The solid lines present the initial ramp-down and dashed lines represent the subsequent ramp-up flow protocol for the same experimental duration. An initial value of $\lambda = 0$ is assigned to the fully letherized state at the initial high shear rate ($\dot{\gamma}_i$). The black hollow circles spaced along the bounding axes represent the trajectory of a sudden flow cessation experiment, in which the shear rate is reduced from $\dot{\gamma}_i$ to $\dot{\gamma}_f$ instantaneously (i.e., the flow is "quenched") and kept at the lowest value for the remainder of the experiment, while monitoring the subsequent recovery in the thixotropy parameter.

Knowing the temporal evolution in the thixotropy parameter $\lambda(My, t)$, one can subsequently compute the expected rheological hysteresis by looking at the evolution in the flow curves for the three different subclasses of thixotropic fluid model (TV, TP, and TVP) summarized above. In Fig. 5, we show the shear stress response of these different models for the same set of ramp-down/ramp-up protocols used for computing the thixotropy parameter presented in Fig. 4. The inset figures show the value of the hysteresis area, $A_\sigma(t_{\mathrm{exp}})$ as the total time of the experiment changes for three different values of $\beta = 0.01,\ 0.1,$ and 1. First, it is clear that all three models robustly predict nonmonotonic hysteretic curves with clear maxima in their distribution of $\tilde{A}_\sigma(t_{\mathrm{exp}})$. This clearly demonstrates that the hysteresis observed in the thixotropy parameter itself is sufficient to lead to rheological hysteresis. For instance, one does not need to necessarily have a yield stress fluid to observe rheological hysteresis (and indeed some complex foodstuffs such as Marmite appear to be *thixoviscous* in nature [50]). However, a closer look shows that the precise form of the constitutive model can substantially change the quantitative characteristics of the $\tilde{A}_\sigma(t_{\mathrm{exp}})$ distributions.

For a given value of β (here taken to be $\beta = 0.1$), we can compare and contrast the hysteresis areas measured from the flow curves for the three different fluids above, as shown in Fig. 6. First it should be noted that, for all three different fluid models considered, the value of the thixotropic time scale in these calculations (held constant here at $\tau_{\mathrm{thix}} = 10\,\mathrm{s}$) differs from the characteristic value of t_{exp} at which the local maximum in the distribution curve of the hysteresis area is observed. This is to be expected because (i) the value of β clearly influences the location of the hysteresis maximum as evident in the inset figures shown in Fig. 5, (ii) for the TV and TVP fluid models, the value of the plastic viscosity can change the exact location of the hysteresis maximum. We also note that in the original step-wise flow protocol described by Divoux *et al.* [25] (and later adapted by [34,36]), the time scale presented on the ordinate axis is the time spent at each shear rate (δt), as opposed to the total time of the experiment ($t_{\mathrm{exp}} = n\delta t$) in our proposed flow protocol. Additionally, one should note that by defining the hysteresis area as given in Eq. (2), the magnitude of the shear stress enters the expression, resulting in larger weighted contributions to the total hysteresis area when thixotropic effects are more pronounced at high shear rates.

If instead computation of the hysteresis area was based (for example) on $\log(\sigma)$ as $A_\sigma = \int_{\dot{\gamma}_f}^{\dot{\gamma}_i} |\Delta \log \sigma(\dot{\gamma})| d \log \dot{\gamma}$, this would shift the location of the maxima in the distribution toward shorter times. For completeness, we show such a plot in the supplementary material [55].

A close inspection of the results for the TP and TV fluid models shows that although the choice of parameters can increase/decrease the total hysteresis area, and the precise value of the experimental time scale at which the maximal hysteresis observed, in general a rather simple distribution with a clear single maximum is measured for each model. This is in agreement with measurements in a range of different

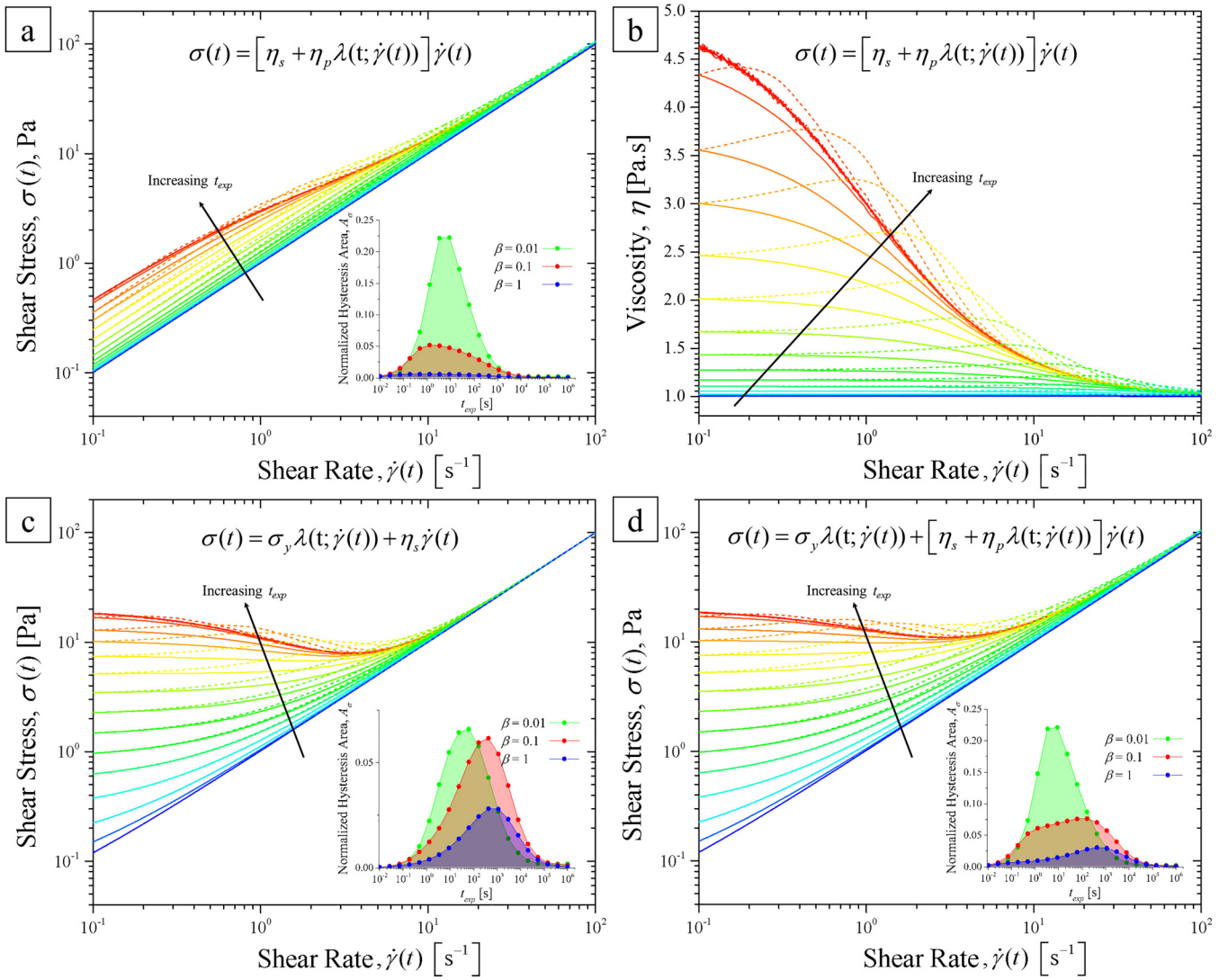

FIG. 5. [(a), (c), and (d)] Expected evolution in the measured shear stress vs applied shear rate, under the ramp-down/ramp-up flow protocol shown schematically in the top row of Fig. 3. Three different types of thixotropic fluid model are considered: [(a) and (b)] TV, (c) TP, and (d) TVP, with constitutive equations for each model shown in the figure, and the results are evaluated numerically using the time-dependent solution for the thixotropy parameter presented in Fig. 4. For clarity in (b), the viscosity of the purely TV fluid is also presented as a function of shear rate, resulting in identical hysteresis loops to those shown in Fig. 3 (due to the linear dependency of the total viscosity on the evolving thixotropy parameter). The color increments from blue to red (see color version online, and indicated in print by the direction of the arrow) in each figure represent longer total times of experiments, t_{exp}, corresponding to different Mu numbers in the range $Mu = 10^{-3}-10^{5}$. The total hysteresis areas $\tilde{A}_\sigma(t_{\text{exp}})$ computed using the expression in Eq. (2) are calculated for different experiment times, and different values of the parameter β, and are presented as inset figures for each constitutive model. The solid lines present the initial ramp-down flow, and the dashed lines represent the ramp-up flow protocols for the same experimental durations.

yield stress materials [25] and also with DPD computations [35]. In contrast, the results for the TVP fluid model show a more complex bimodal distribution with distinct contributions from both the viscous and the plastic contributions to the total stress. Other more sophisticated models such as those proposed by Geri *et al.* [45], Larson [10,26], and a population balance model proposed by Mwasame *et al.* [51], in which different microscopic physical processes (with different characteristic time scales) give rise to different contributions to the total stress will also predict a similar multimodal response.

Because of this difficulty in directly recovering the precise numerical value of the thixotropic time scale (which in the three models considered here is of course known *a priori*) from hysteresis area measurements, we propose augmenting the ramp-down/ramp-up protocol with one simple final additional step; i.e., a sudden cessation or "quench" of the system from an initially letherized state [corresponding to a long time of shearing at a high shear rate $\dot{\gamma}_i$ (i.e., $Mu \gg 1$ and $My \gg 1$)] to the lowest possible final experimentally resolvable (nonzero) shear rate ($\dot{\gamma}_f$), and directly monitoring the recovery in the shear stress as the microstructure rebuilds. We perform this stress jump experiment numerically with a very short ramp down protocol (corresponding to $t_{\text{exp}} = 0.1$ s) followed by 100 s of steady shear flow at a constant shear rate of $\dot{\gamma}_f = 0.1\ \text{s}^{-1}$. Results of such a quench/recovery protocol are presented as the hollow black solid circles in Fig. 4 [holding the shear rate at a constant low (but nonzero) value results in evolution of the thixotropy parameter in a vertical fashion along the ordinate axis when results are plotted vs the applied shear rate]. The same results are presented against time in Fig. 7 and show a smooth monotonic recovery in the structure and, thus, in the shear stress of the material as well.

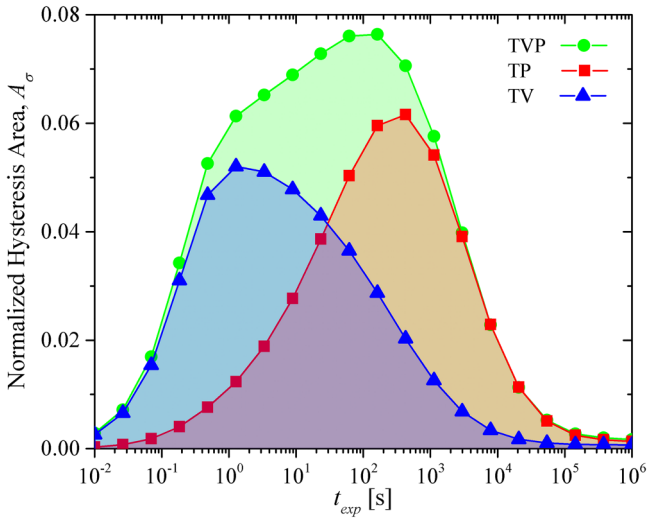

FIG. 6. Total rheological hysteresis computed for the three different types of inelastic thixotropic fluid models, all with the same constant values of $\beta = 0.1$ and $\tau_{\text{thix}} = 10\,\text{s}$ in Eq. (2).

Equation (2) can also be solved analytically using an integrating factor when the shear history $\dot{\gamma}(t)$ is specified. For the simplest case, when a constant shear rate of strength $\dot{\gamma}_f$ is applied, this results in the following expression:

$$\lambda(t;\dot{\gamma}_f) = \frac{1}{1+\beta\dot{\gamma}_f\tau_{\text{thix}}} - \left(\frac{1}{1+\beta\dot{\gamma}_f\tau_{\text{thix}}} - \lambda_0\right) e^{-(1+\beta\dot{\gamma}_f\tau_{\text{thix}})t/\tau_{\text{thix}}}, \qquad (4)$$

where λ_0 indicates the nonzero (but typically negligibly small) residual value of the thixotropy parameter in the fully

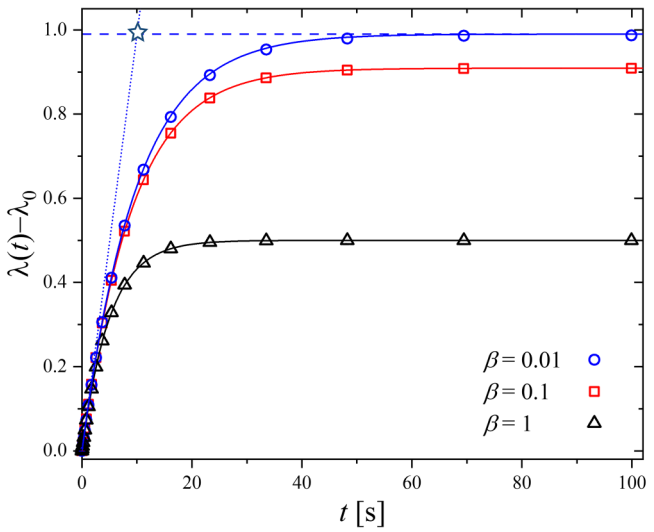

FIG. 7. The evolution of the thixotropy parameter, λ, with total elapsed time of experiment for a very rapid quench/recovery (i.e., a stress jump-down experiment). The hollow circles represent the numerical solution of Eq. (2) and the solid line represents the analytical solution given in Eq. (3). The hollow star indicates the intersection of the asymptotic value of $\lambda(\dot{\gamma}_f, t\to\infty) = 1/[1+\beta\dot{\gamma}_f\tau_{\text{thix}}]$ (blue dashed line) and the Taylor series expansion of Eq. (3) (blue dotted line). Provided $My_f \ll 1$ this gives a good direct estimate of the thixotropic time scale, as shown by the blue dashed line.

letherized state at $My_i \gg 1$. The expression in Eq. (4) is shown in Fig. 7 by the solid lines. The asymptotic value of λ at long times depends on the parameter β (as evident from the figure) and is given by $\lambda(\dot{\gamma}_f, t\to\infty) = 1/(1+\beta\dot{\gamma}_f\tau_{\text{thix.}}) = 1/(1+\beta My_f)$. The blue dotted line represents the Taylor series expansion series of Eq. (3) at short times. Solving for the intersection point of the Taylor series expansion at short time and the asymptotic value of λ at long time gives the following expression:

$$t^* \cong \frac{\tau_{\text{thix}}}{1+\beta My_f}, \qquad (5)$$

which provides a very easy method for recovering the thixotropic time scale τ_{thix} (as indicated by the hollow star shown in Fig. 7).

V. DISCUSSION AND CONCLUSIONS

In this article, we have proposed a framework and language for quantifying the magnitude of thixotropic effects in complex fluids under steady and time-varying shear flows. We believe the definition and reporting of a *Mnemosyne number*, $My = \tau_{\text{thix}}\dot{\gamma}$ (to quantify the relative magnitude of thixotropic effects), as well as a *mutation number* $Mu = t_{\text{exp}}/\tau_{\text{thix}}$ (to report the duration of a particular test protocol or flow process) will help rheologists unravel and understand the complexities of thixotropic effects in complex fluids. We have outlined several possible rheometric test protocols that enable the thixotropic time scale and the magnitude of the rheological hysteresis in a given material to be quantified in a convenient manner for experimentalists and theoreticians alike. The ramp-down/ramp-up protocol corresponds to a series of up/down vertical trajectories through the *Mu–My* state space sketched in Fig. 1. There are, of course, many other putative test protocols that can be proposed to explore this space (for example, exponential ramps down/up [35], or a staircase series of constant rates that are stepped down/up [25]) and the optimal protocol may be expected to vary for diverse systems ranging from consumer products to foods comprised of structured pastes or jammed emulsions. However, all such protocols can be represented in the *Mu–My* state space, and the fully "shear-melted" or destructured material state—in which memories of all previous deformation histories are eliminated—is always clearly represented by the fully *letherized* state located in the upper right of this diagram. Finally, we note that for more complex TEVP material systems (e.g., many colloidal gels) which show rheological aging, and/or pronounced viscoelastic effects, this two-dimensional state space must also be augmented with additional dimensions (capturing the material age and the viscoelastic relaxation time, respectively).

The thermal analogy hinted at by the term "shear-melting" is a useful one to investigate further in the future. When converted to a proper frame-invariant form (i.e., by replacing the ordinary time derivative with a material derivative, $D\lambda/Dt$), the evolution equations considered here for the scalar order parameter $\lambda(t)$ resemble transport equations for other passive scalars such as a (suitably nondimensionalized) temperature

field, $\theta(t)$. Many of the tools and analyses developed for quantifying thermal entrance lengths and describing the evolution of thermal boundary layers may thus be adapted to future studies of thixotropic flows in more complex geometries. As a specific example, the pressure-driven flow of an initially fully restructured material (i.e., a material with $\lambda = 1$) from a tank or reservoir into a narrow slit or pipe is closely analogous to the entrance flow of a cold fluid into a hot-walled tube or (even more closely) to a viscous heating problem such as that studied by Dinh and Armstrong [52]. In this latter problem, the high shear rates experienced by the fluid elements near the wall locally increase the temperature of the fluid (or, equivalently, in the case of a thixotropic fluid, locally destructures the material). In each case, the question of interest is what is the steady-state spatial distribution of the temperature field across the channel $T(x,y)$ or equivalently the level of structure $\lambda(x, y)$ in a thixotropic material that is sensitive to its entire shear history. Material elements moving along different streamlines experience different mutation numbers and Mnemosyne numbers and, therefore, different levels of sensitivity to the effects of thixotropy. One important distinction between the thermal problem and the naïvest thixotropic transport equation, such as Eq. (3), is the absence of a diffusive term (of the form $\nabla^2\lambda$) that is necessary to establish a balance between convection in the flow direction and diffusion normal to the bounding walls. The important role of such nonlocal terms has been considered, in the context of thixotropy and hysteresis loops specifically, by Radhakrishnan *et al.* [34] for example.

In this Perspective, we have only analyzed simple models in which a single thixotropic time scale is relevant, while in virtually all real thixotropic systems, a spectrum of time scales is present, as shown in the recent work of Sen and Ewoldt [53], which can be described through a series of λ_j which all undergo evolution in time [26]. For systems in which distinct time scales are measurable, different *Mu* numbers can be defined to emphasize the range of time scales involved for the corresponding underlying microstructural elements. For example, it is certainly possible for any of the simple structural models that we use to illustrate our ideas to define two different Mnemosyne numbers depending on whether we base it on the restructuring time scale (τ_{thix}) or the breakdown time scale which we write as $\beta\tau_{\text{thix}}$, but other authors may just write as two rate constants, k_1 and k_2 [which typically have different physical units, depending on the precise functional form of the breakdown term in Eq. (3)], respectively. Here, we argue that a natural way of measuring τ_{thix} is through measurements of the shear stress recovery following a quench experiment from a high shear rate flow to a low (but nonzero) shear rate, and it is thus most appropriate to base the definition of *My* on this restructuring time scale; however, a second Mnemosyne number can then be clearly written as the product of two dimensionless groups $\beta.My$. This is completely analogous to the way polymer rheologists define Weissenberg numbers based on either the Rouse or the reptation time scale, but then interrelate them by noting that $Wi_{\text{Rouse}} = Wi_{\text{rep}}/3Z$, where Z is the number of entanglements. In reptation theories, the dimensionless parameter Z represents a dimensionless ratio of the tube orientation time scale to the chain stretching time scale. Equivalently, in thixotropy models, the dimensionless parameter β represents a ratio of the structure break-down to restructuring time scales. Whichever choice of a mean/average structural time scale is preferred in a specific problem, a Mnemosyne number can always be clearly defined and used to construct *Mu–My* maps for exploring and understanding the complex time-dependent response of thixotropic material systems.

Agarwal *et al.* [13] have recently argued for other shearing protocols (such as step strains imposed after cessation of preshearing with different waiting times, t_w) that can distinguish between rheological aging and nonlinear viscoelasticity, and it will be interesting to represent the resulting material hysteresis in plots of the type we show in Figs. 5 and 6 where the appropriate mutation number now becomes $Mu = t_w/\tau_{\text{thix}}$.. Stadler *et al.* [54] have also recently proposed a series of interval experiments for thixotropic characterization of emulsions and colloidal systems. Thixotropy will again correspond to nonmonotonic measures of hysteresis at time scales that are generally much longer than similar measurements originating from nonlinear viscoelastic effects.

Finally, it should be emphasized that it is only for didactic simplicity that we focused here exclusively on inelastic models. This enables us to illustrate our key conceptual ideas using the most elementary constitutive models possible. As noted in Sec. I, in most real-world systems (such as consumer products, paints, inks, and foodstuffs) at least some level of material viscoelasticity is also present [as detectable, for example, by non-zero values of $G'(\omega)$—which of course are identically zero for the models we consider] and more realistic constitutive models must account for both viscoelastic and thixotropic time scales/constituents. This inevitably leads to more material parameters, as well as the need to represent the dynamical response of the system in a higher-dimensional space; this can readily be done and in the future may be represented unambiguously in terms of a Weissenberg number plus a mutation number and a Mnemosyne number.

ACKNOWLEDGMENTS

Complex fluids research in the Non-Newtonian Fluids (NNF) group at MIT is supported by a gift from Procter & Gamble. Many of the underlying ideas in this perspective originated through discussions between the authors during the course of flow assurance research supported by Chevron ETC, Houston. The authors would also like to acknowledge extensive and often spirited discussions with R. Ewoldt, T. Divoux, D. Vlassopoulos, M. Denn, and Y. Joshi.

AUTHOR DECLARATIONS

Conflict of Interest

The authors have no conflicts to disclose.

REFERENCES

[1] Reiner, M., "The Deborah number," Phys. Today **17**(1), 62 (1964).
[2] Dealy, J. M., "Weissenberg and Deborah numbers—Their definition and use," Rheol. Bull. **79**(2), 14–18 (2010).

[3] White, J. L., "Dynamics of viscoelastic fluids, melt fracture, and the rheology of fiber spinning," J. Appl. Polym. Sci. **8**(5), 2339–2357 (1964).
[4] Porteous, K. C., and M. M. Denn, "Linear stability of plane Poiseuille flow of viscoelastic liquids," Trans. Soc. Rheol. **16**(2), 295–308 (1972).
[5] Wagner, N. J., and J. F. Brady, "Shear thickening in colloidal dispersions," Phys. Today **62**, 27–32 (2009).
[6] Barnes, H. A., "Thixotropy—A review," J. Non-Newtonian Fluid Mech. **70**(1), 1–33 (1997).
[7] Mewis, J., "Thixotropy—A general review," J. Non-Newtonian Fluid Mech. **6**(1), 1–20 (1979).
[8] Mewis, J., and N. J. Wagner, "Thixotropy," Adv. Colloid Interface Sci. **147–148**, 214–227 (2009).
[9] Larson, R. G., "Constitutive equations for thixotropic fluids," J. Rheol. **59**(3), 595–611 (2015).
[10] Larson, R. G., and Y. Wei, "A review of thixotropy and its rheological modeling," J. Rheol. **63**(3), 477–501 (2019).
[11] Cheng, D. C., "Thixotropy," Int. J. Cosmet. Sci. **9**(4), 151–191 (1987).
[12] de Souza Mendes, P. R., and R. L. Thompson, "Time-dependent yield stress materials," Curr. Opin. Colloid Interface Sci. **43**, 15–25 (2019).
[13] Agarwal, M., S. Sharma, V. Shankar, and Y. M. Joshi, "Distinguishing thixotropy from viscoelasticity," J. Rheol. **65**(4), 663–680 (2021).
[14] Bauer, W. H., and E. A. Collins, "Chapter 8—Thixotropy and dilatancy," in *Rheology*, edited by F. R. Eirich (Academic, New York, 1967), pp. 423–459.
[15] Péterfi, T., "Die abhebung der Befruchtungsmembran bei seeigeleiern," Wilhelm Roux'Arch. Entwicklungsmech. Org. **112**(1), 660–695 (1927).
[16] Mewis, J., and N. J. Wagner, *Colloidal Suspension Rheology*, Cambridge Series in Chemical Engineering (Cambridge University, New York, 2012).
[17] Wagner, N. J., and J. Mewis, *Theory and Applications of Colloidal Suspension Rheology* (Cambridge University, Cambridge, 2021).
[18] Schalek, E., and A. Szegvari, "Die langsame koagulation konzentrierter eisenoxydsole zu reversiblen gallerten," Kolloid-Zeitschrift **33**(6), 326–334 (1923).
[19] Freundlich, H., "Ueber thixotropie," Kolloid-Zeitschrift **46**(4), 289–299 (1928).
[20] Hauser, E., "Über die thixotropie von dispersionen geringer konzentration," Kolloid-Zeitschrift **48**(1), 57–62 (1929).
[21] Coleman, B. D., and W. Noll, "Foundations of linear viscoelasticity," Rev. Mod. Phys. **33**(2), 239–249 (1961).
[22] Green, H., and R. Weltmann, "Analysis of thixotropy of pigment-vehicle suspensions—Basic principles of the hysteresis loop," Ind. Eng. Chem., Anal. Ed. **15**(3), 201–206 (1943).
[23] Bird, R. B., and B. D. Marsh, "Viscoelastic hysteresis. Part I. Model predictions," Trans. Soc. Rheol. **12**(4), 479–488 (1968).
[24] Fredrickson, A. G., *Principles and Applications of Rheology* (Prentice-Hall, Englewood Cliffs, 1964).
[25] Divoux, T., V. Grenard, and S. Manneville, "Rheological hysteresis in soft glassy materials," Phys. Rev. Lett. **110**(1), 018304 (2013).
[26] Wei, Y., M. J. Solomon, and R. G. Larson, "Letter to the editor: Modeling the nonmonotonic time-dependence of viscosity bifurcation in thixotropic yield-stress fluids," J. Rheol. **63**(4), 673–675 (2019).
[27] Varchanis, S., G. Makrigiorgos, P. Moschopoulos, Y. Dimakopoulos, and J. Tsamopoulos, "Modeling the rheology of thixotropic elasto-visco-plastic materials," J. Rheol. **63**(4), 609–639 (2019).
[28] Ewoldt, R. H., and G. H. McKinley, "Mapping thixo-elasto-visco-plastic behavior," Rheol. Acta **56**(3), 195–210 (2017).
[29] Eliade, M., "Mythologies of memory and forgetting," Hist. Relig. **2**(2), 329–344 (1963).
[30] Mours, M., and H. H. Winter, "Time-resolved rheometry," Rheol. Acta **33**(5), 385–397 (1994).
[31] Geri, M., B. Keshavarz, T. Divoux, C. Clasen, D. J. Curtis, and G. H. McKinley, "Time-resolved mechanical spectroscopy of soft materials via optimally windowed chirps," Phys. Rev. X **8**(4), 041042 (2018).
[32] Pryce-Jones, J., "Experiments on thixotropic and other anomalous fluids with a new rotation viscometer," J. Sci. Instrum. **18**(3), 39–48 (1941).
[33] Choi, J., M. Armstrong, and S. A. Rogers, "The role of elasticity in thixotropy: Transient elastic stress during stepwise reduction in shear rate," Phys. Fluids **33**(3), 033112 (2021).
[34] Radhakrishnan, R., T. Divoux, S. Manneville, and S. M. Fielding, "Understanding rheological hysteresis in soft glassy materials," Soft Matter **13**(9), 1834–1852 (2017).
[35] Jamali, S., R. C. Armstrong, and G. H. McKinley, "Time-rate-transformation framework for targeted assembly of short-range attractive colloidal suspensions," Mater. Today Adv. **5**, 100026 (2020).
[36] Jamali, S., R. C. Armstrong, and G. H. McKinley, "Multiscale nature of thixotropy and rheological hysteresis in attractive colloidal suspensions under shear," Phys. Rev. Lett. **123**(24), 248003 (2019).
[37] Ong, E. E. S., S. O'Byrne, and J. L. Liow, "Yield stress measurement of a thixotropic colloid," Rheol. Acta **58**(6), 383–401 (2019).
[38] Rathinaraj, J. D. J., J. Hendricks, G. H. McKinley, and C. Clasen, "Orthochirp: A fast spectro-mechanical probe for monitoring transient microstructural evolution of complex fluids during shear," J. Non-Newtonian Fluid Mech. **301**, 104744 (2022).
[39] Helal, A., T. Divoux, and G. H. McKinley, "Simultaneous rheoelectric measurements of strongly conductive complex fluids," Phys. Rev. Appl. **6**(6), 064004 (2016).
[40] Goodeve, C. F., "A general theory of thixotropy and viscosity," Trans. Faraday Soc. **35**, 342–358 (1939).
[41] Coussot, P., Q. D. Nguyen, H. T. Huynh, and D. Bonn, "Viscosity bifurcation in thixotropic, yielding fluids," J. Rheol. **46**(3), 573–589 (2002).
[42] Bird, R. B. *et al.*, *Dynamics of Polymeric Liquids, Volume 2: Kinetic Theory* (Wiley, New York, 1987).
[43] Dimitriou, C. J., and G. H. McKinley, "A comprehensive constitutive law for waxy crude oil: A thixotropic yield stress fluid," Soft Matter **10**(35), 6619–6644 (2014).
[44] Armstrong, M. J., A. N. Beris, S. A. Rogers, and N. J. Wagner, "Dynamic shear rheology of a thixotropic suspension: Comparison of an improved structure-based model with large amplitude oscillatory shear experiments," J. Rheol. **60**(3), 433–450 (2016).
[45] Geri, M., R. Venkatesan, K. Sambath, and G. H. McKinley, "Thermokinematic memory and the thixotropic elasto-viscoplasticity of waxy crude oils," J. Rheol. **61**(3), 427–454 (2017).
[46] de Souza Mendes, P. R., "Thixotropic elasto-viscoplastic model for structured fluids," Soft Matter **7**(6), 2471–2483 (2011).
[47] Le-Cao, K., N. Phan-Thien, N. Mai-Duy, S. K. Ooi, A. C. Lee, and B. C. Khoo, "A microstructure model for viscoelastic–thixotropic fluids," Phys. Fluids **32**(12), 123106 (2020).
[48] Fredrickson, A. G., "A model for the thixotropy of suspensions," AIChE J. **16**(3), 436–441 (1970).
[49] Blackwell, B. C., and R. H. Ewoldt, "A simple thixotropic–viscoelastic constitutive model produces unique signatures in large-amplitude oscillatory shear (LAOS)," J. Non-Newtonian Fluid Mech. **208–209**, 27–41 (2014).

[50] White, D. E., G. D. Moggridge, and D. Ian Wilson, "Solid–liquid transitions in the rheology of a structured yeast extract paste, Marmite™," J. Food Eng. **88**(3), 353–363 (2008).

[51] Mwasame, P. M., A. N. Beris, R. B. Diemer, and N. J. Wagner, "A constitutive equation for thixotropic suspensions with yield stress by coarse-graining a population balance model," AIChE J. **63**(2), 517–531 (2017).

[52] Dinh, S. M., and R. C. Armstrong, "Non-isothermal channel flow of non-Newtonian fluids with viscous heating," AIChE J. **28**(2), 294–301 (1982).

[53] Sen, S., and R. H. Ewoldt, "Thixotropic spectra and Ashby-style charts for thixotropy," arXiv:2201.10004 (2022).

[54] Stadler, F. J. *et al.*, "Multiple interval thixotropic test (miTT)—An advanced tool for the rheological characterization of emulsions and other colloidal systems," Rheol. Acta **61**, 229–242 (2022).

[55] See supplementary material at https://www.scitation.org/doi/suppl/10.1122/8.0000432 for additional results for similar sweeping ramp down/up flow protocols as studied in the manuscript but instead using a Coussot-Bonn viscosity-bifurcating constitutive model.